Supporting Information

In situ investigation on the formation and metastability of formamidinium lead tri-iodide perovskite solar cells

Jeffery A. Aguiar[1*,§], Sarah Wozny[2,§], Terry Holesinger[3], Toshihiro Aoki[4], Maulik K. Patel[5], Mengjin Yang[1], Joseph Berry[1], Mowafak. Al-Jassim[1], Weilie Zhou[2*], and Kai Zhu[1*]

[1] National Renewable Energy Laboratory, Golden, CO, 80401, USA

[2] Advanced Materials Research Institute, University of New Orleans, New Orleans, LA, 70148, USA

[3] Los Alamos National Laboratory, Los Alamos, NM, 80465, USA

[4] Arizona State University, LeRoy Eyring Center for Solid State Science, Tempe, AZ, 85287, USA

[5] Department of Materials Science and Engineering, University of Tennessee, Knoxville, TN, 37996, USA

* Corresponding authors:

J.A.A. E-mail: jeffery.aguiar@nrel.gov, tel: +1 (303) 384-6485.

W.Z. E-mail: wzhou@uno.edu, tel: +1 (504) 280-1068

K.Z. E-mail: Kai.Zhu@nrel.gov, tel: +1 (303) 384-6353

§ Joint authorship

Scanning Transmission Electron Microscopy

Energy filtered aberration corrected high resolution STEM imaging was performed using monochromated Nion Ultra STEM equipped with a cold-field emission gun as the electron source and capable of spherical aberration correction of the third and fifth order aberrations. The STEM was operated at 40 and 60 kV with less than 10 pA beam current, which is below the knock-off damage of most carbon-based materials, including graphene. Low (BF), medium (MAADF), and high angle annular dark field (HAADF) STEM 1024 x 1024 pixel images were acquired with a convergence of 30 mrad and a collection semi-angle of 50-200 mrad with a 3 us

dwell time. Multiple raw images were collected, cross correlated, and summed over a period of 5 mins to minimize beam dose. The samples were imaged with less than 64 e-/nm^2 per frame. Prior to STEM, the perovskite specimens were annealed at 170ºC for 10 mins and then placed in a dedicated double tilt.

High Resolution Valence Electron Energy Loss Spectroscopy

All valence electron energy loss spectra (VEELS) were taken in Scanning Transmission Electron Microscopy (STEM) mode. Ångström sized probes were used with Full-Width Half-Maxima (FWHM) of the ZLP ranging nearly 20 meV for 1s spectrum acquisitions. The microscope used for this study was specifically chosen to capture the valence nature of perovskite materials. The cold Field Emission Gun (FEG) of the Nion UltraSTEM was operated at 60 kV and 40 kV acceleration voltages with a 30 mrad probe convergence and 45 mrad collection angle at 60 kV. These conditions provide the best native energy spread of nearly 10-20 meV, based on the zero-loss peak FWHM, measured with 0.02 eV/pixel dispersion through a large solid acceptance angle into the spectrometer which was obtained with a reduced extraction voltage resulting in a probe current of about 8 pA, resulting in beam dose less than 64 e-/nm^{2}s. For imaging, a 30mrad convergence semiangle was used. VEELS collection was performed with a 12 mrad convergence semiangle and 15mrad EELS collection angle.

Gentle beam conditions and multiple frame acquisition was performed following the routines and discussions in the open literature. [1-3] Beam focusing was further checked to assure proper alignment into the spectrometer aperture opening. Spectra were then analyzed and processed to subtract residual background associated with sampling on a silicon nitride substrate. To perform the subtraction, several raw silicon nitride, vacuum zero loss, and dark count reference VEELS profiles were collected at the same time of collection. The scaled zero-loss peak subtraction routine outlined in Aguiar *et al.* was then applied to resolve subtracted spectra profiles[4]. Subtraction of the silicon nitride signal was then performed via the same technique, where the silicon nitride VEELS subtracted profiles where fit against collected perovskite VEELS profiles. The subsequent subtraction resolves the perovskite or grain boundary only signal VEELS profiles, shown in the main text.

in-situ Gas Experiments

The in-situ gas cell is comprised of a silicon microchip and silicon nitride viewing membrane that forms a viewing port. For our experiments, 25 nm thick silicon nitride windows were used. The perovskite material was dropped on onto a titania and UV treated silicon nitride space chip. The silicon nitride spacer chip thereby was made up of the following layering: perovskite/mesoporous titania/amorphous silicon nitride. The treated chip was then placed into the Hummingbird Scientific in-situ heated gas holder. A calibrated silicon heating chip was then placed face-to-face with the treated silicon nitride spacer. Once positioned into the holder, the system was sealed using O-ring seals, a cover plate, retention clip, and then secured with a single setscrew. The system was then leak checked to ensure high vacuum could be attained using in a dry pump vacuum station. Following leak testing argon gas was also delivered to the system to

check the vacuum seals under pressure. The system was then placed in a transmission electron microscope. Before observation, argon gas was delivered to the gas cell using hard metallic tubing to deliver and flush the cell for 30 min prior to heating and transmission electron microscopy. During this time the cell was checked for leaks. The process is further illustrated in Figure S1. A treated silicon nitride window with compact titania is also imaged shown in Figure S2, using TEM, which forms the growth template for our subsequent in-situ crystallization studies

in-situ (Scanning) Transmission Electron Microscopy

Simultaneously with the in-situ heating gas experiments, bright field (BF), annular dark field (ADF), selected area electron diffraction (SAED), and transmission electron micrographs were recorded using an aberration-corrected FEI Titan S/TEM and FEI Tecnai. Prior to observation the specialized *in situ* gas holder was initially purged and filled internally. Observation of the material was performed while flowing argon gas. The ADF and BF STEM images were collected on the Cs aberration-corrected FEI Titan S/TEM operated at 300 kV using a Fischione model 3000 high angle annular dark field STEM detector and the annular bright field STEM images were acquired using the Gatan camera with Gatan Digital Micrograph software. The following imaging conditions were used for ADF STEM imaging: 40kx magnification, -0.050 um defocus, 70 mm final probe forming condenser aperture, 100 mm nominal camera length, roughly 1.6 Å probe diameter, 0.030 nA probe current, 42.9 mrad convergence semi-angle and 55–330 mrad inner and outer collection semi-angle, an image size of 2048 x 2048 pixels, 871 pm x 871 pm pixel size, 1.78 μm x 1.78 μm small area, 1 μs pixel dwell time, and with a 4.34 s total frame time. The total incident electron beam dose was 256.37 e-/nm^2 per frame. One frame was collected at each snapshot. Images were time stamped and recorded initially, and then stacked to form movie-like snapshots.

Chemical Spectral Imaging

Complementary, composite spectral imaging using STEM-based energy dispersive x-ray spectroscopy was performed on an as-completed perovskite film in planar view on silicon nitride. To resolve the final chemistry, the perovskite sample was loaded on a single tilt low background holder and placed in the aberration corrected FEI Titan operated and a significant monochromated defocus was used to reduce the beam current. A host of composite chemical images, where then performed including both line and two-dimensional line scans. Figure S3 is a resultant composite chemical images profiling one of our annealed PSC films grown through sequential annealing. Due to associated sample thickness, however, based on these series of experiments, shown in Figure S4, we are confident in the annealed chemistry of our perovskite thin films.

Grazing Incidence X-ray Diffraction

Grazing incidence x-ray diffraction (GXRD) measurements were performed using a Panalytical X'Pert^3 MRD X-ray diffractometer equipped with Cu K-α source (1.54059 Å) radiation and a Xe-proportional detector. The GXRD patterns were recorded in a 2θ scanning mode using a parallel beam mirror on the incident beam side and a parallel plate collimator of 0.27 divergence on the diffracted beam side. A combination of beam mask and divergence slits was selected to illuminate the sample surface without illuminating the sample holder. The GXRD patterns were collected in the 2θ range between 10-90° with a step size of 0.02° and step time of 1 sec/step. Profiling several as-grown perovskite materials as shown in Figure S5, clearly resolves the presence of the following materials: $HC(NH_2)_2PbI_3$ (host perovskite material), PbI_2 (signature of grain boundary segregation), TiO_2 (compact growth layer), and soda lime-glass (substrate).

in-situ Selected Area Electron X-ray Diffraction

Complementary to the *in-situ* XRD, **Figure S3** and **S4** are a complementary structural timeline focused on the formation of $FAPbI_3$ by collecting selected area electron diffraction (SAED) using identical imaging (300 kV, 10 um^2 area, 468 e-/nm^{2}f) and sample conditions to the *in-situ* imaging study. The SAED diffraction profiles were performed using an azimuthal integration of the original 2-dimensional diffraction pattern and indexed against PbI_2 (blue), $FAPbI_3$ (black) and the Si_3N_4 chip (red). In light of the the effects of texturing and overlapping peaks, we can ascertain that between 125° C and 150° C the diffraction perovskite peaks at approximately 1.7 Å and 2.25 Å form with nearly equal intensity. This is complementary and supports the *in-situ* imaging and XRD which benefits from higher resolution and shows the same trend in the formation of perovskite material between the techniques. Given the agreement between the multiple datasets, suggests there are minimal effects of electron beam dose.

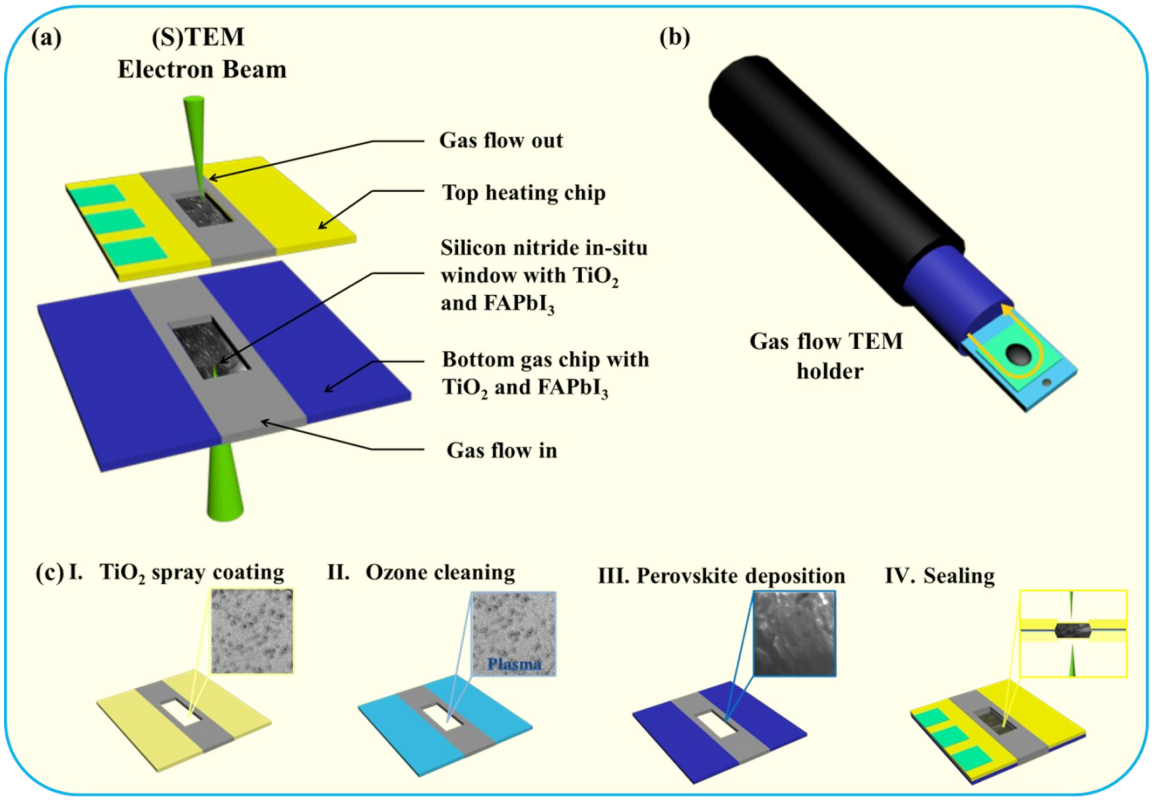

Figure S1 : Schematic of the experimental design: **(a)** Schematic of the heated in-situ gas cell used for the controlled temperature study of FA-based PSCs inside with heating capability from 50°C to 225°C while flowing inert argon gas; **(b)** Schematic of the gas flow holder; and **(c)** schematic of the step by step sealing of the silicon nitride microchips.

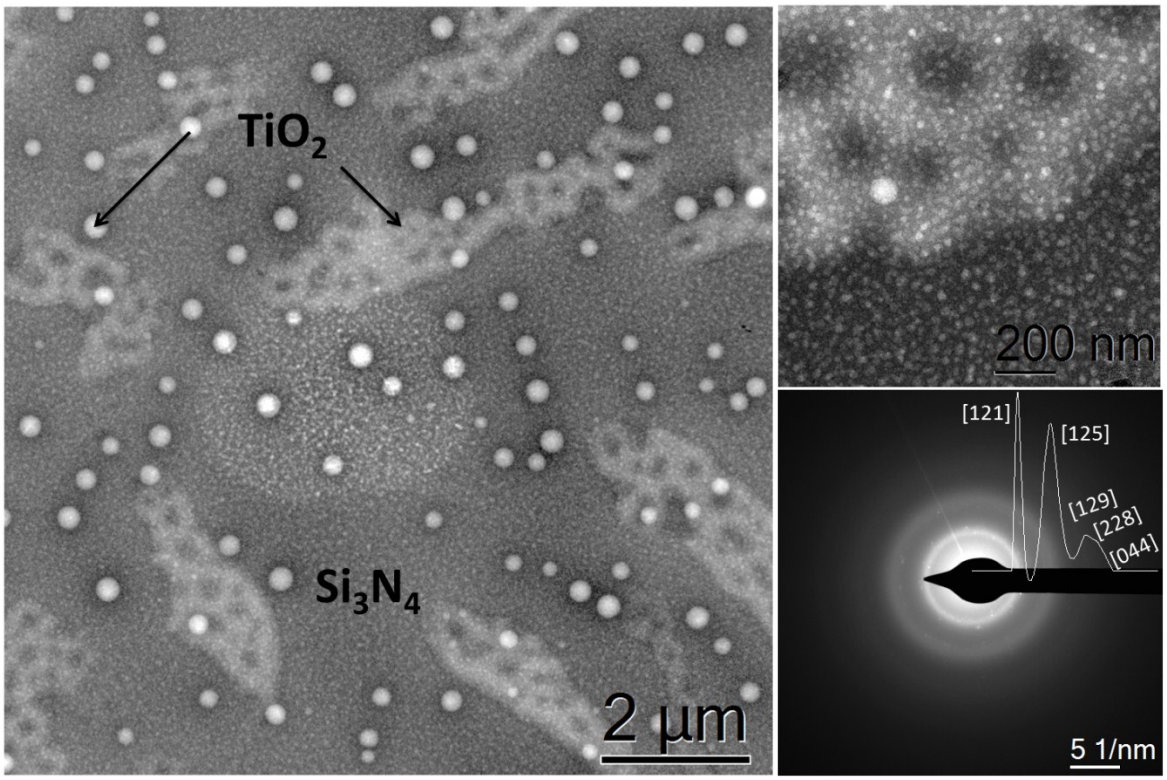

Figure S2: (a) Low magnification TEM image of TiO_x compact layer spray coated on the silicon nitride microchip. The bright and spotted areas correspond to spray coated compact titania on darker amorphous silicon nitride window. **(b)** Higher magnification image of the same area shows titania nanocrystals with a size between 10 and 20 nm. **(c)** SAED profiling confirms the presence of the TiO_x compact thin film on amorphous silicon nitride substrate.

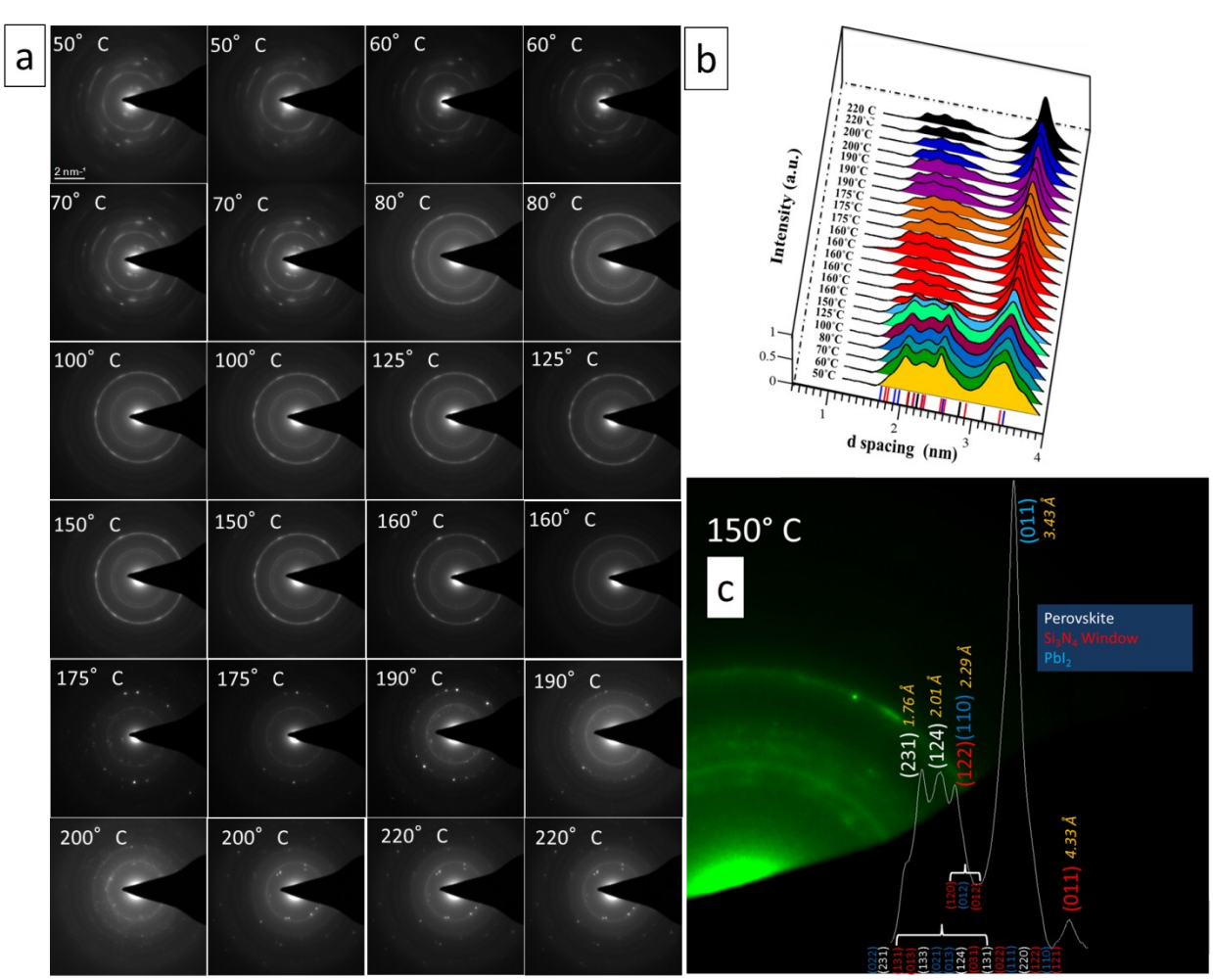

Figure S3: (a) Complementary, collected polycrystalline diffraction ring patterns, tracking the same reported diffraction profiles reported in Figure 1d, displayed here as waterfall plot **(b)** with the crystallographic lattice spacings for perovskite (black lines), silicon nitride (red), and lead iodide (blue). There are two polycrystalline diffraction snapshots per temperature. Each corresponds to the beginning and end of the temperature sequence depicted in the temperature profile (Figure 1b). **(c)** Indexing the individual peaks on the SAED is difficult, however we shown for one temperature (150° C) the overlay the crystallographic peaks and highlighted the major peaks with the corresponding azimuthal projection. Above 160° C, we begin to also lose the nanocrystallinity (i.e. diffraction rings) associated with the material.

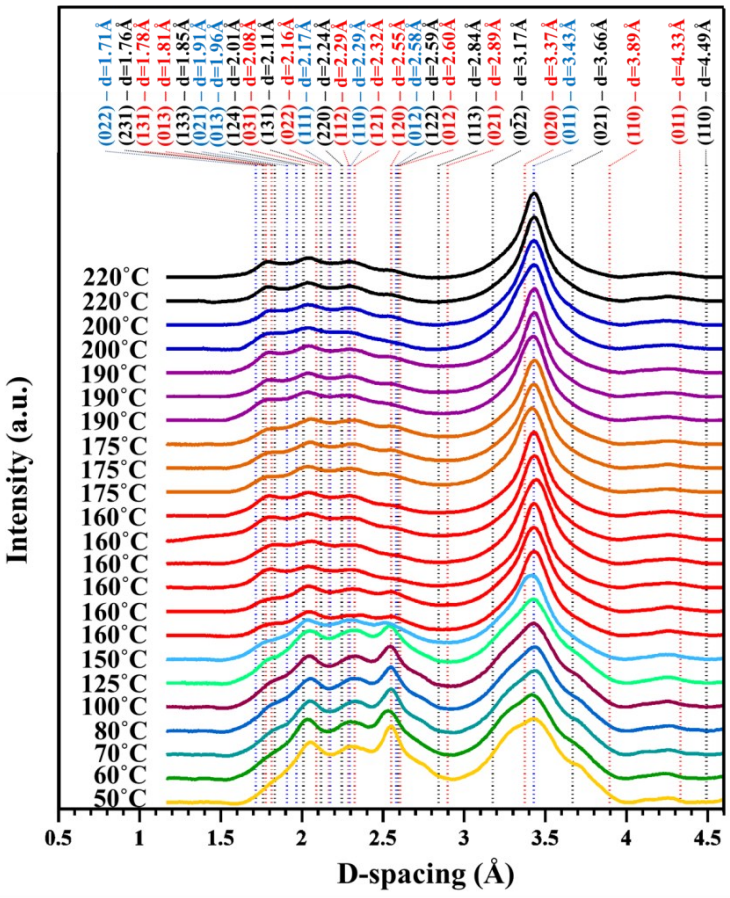

Figure S4: Azimuthal projected SAED profiles collected from the polycrystalline diffraction ring patterns, tracking the same temperatures in Figure 1b.

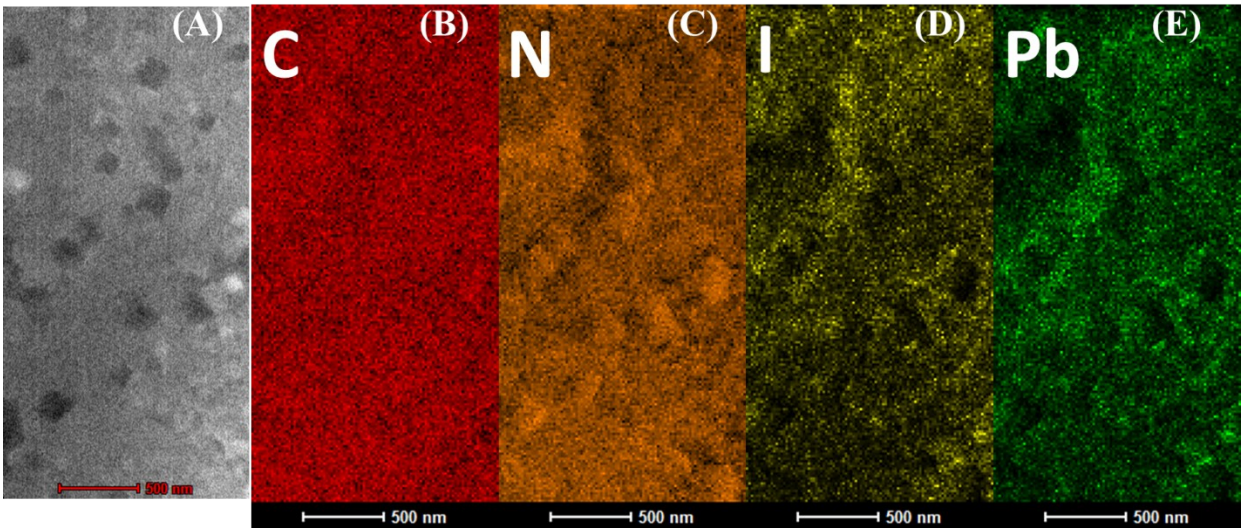

Figure S5: (a) Complementary, use of STEM-based EDS imaging and **(b-d)** chemical imaging provides a final snapshot of one of our reacted and annealed perovskite thin-films. This material is a planar view perspective of a thick textured perovskite film grown on compact titania and silicon nitride. The white and dark contrast corresponds to a final convolution of the deposited thick film texture (where HAADF is also sensitive to mass thickness variation) as well as the presence of perovskite and lead. From our post-chemical analyses we are able to qualitatively image **(b)** C-*K*, **(c)** N-*K*, **(d)** I-*L*, and **(e)** Pb-*M* x-ray lines, where quantitatively it is difficult to detect individual grains due to the mixed morphology of the as grown thick annealed perovskite layer, as mentioned previously. Cross-sectional TEM imaging is also not possible due to the beam sensitive nature of the sample. This however is complementary analysis clearly resolving a lead containing species segregates species to grain boundaries.

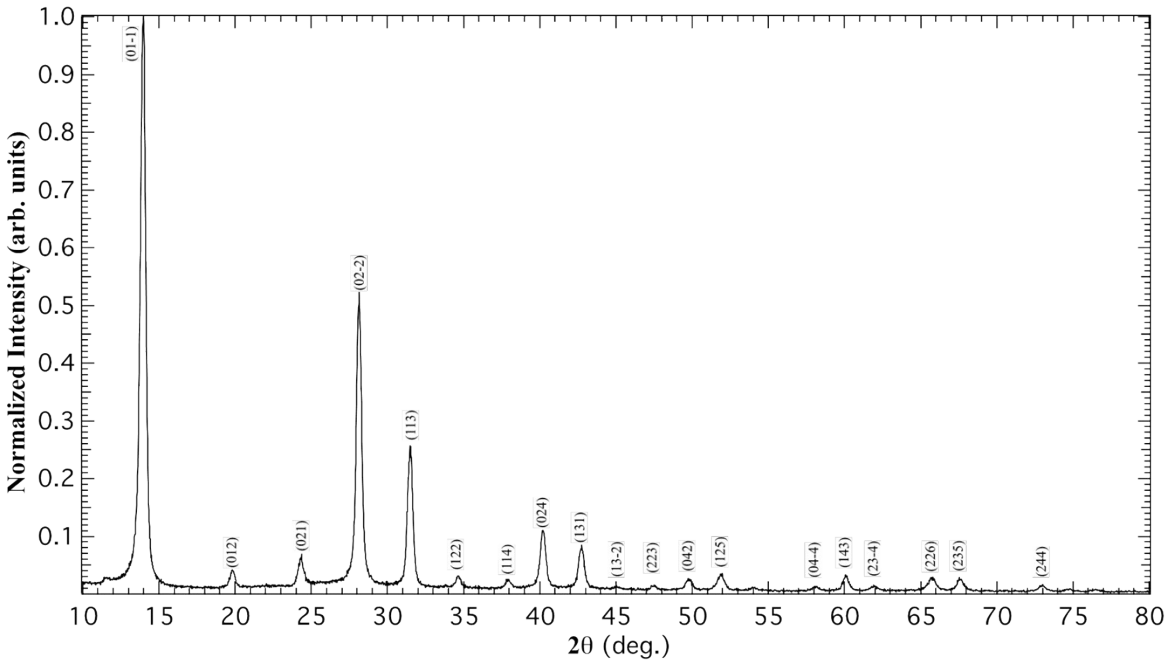

Figure S6: Grazing incidence XRD confirms alpha phase FA-based perovskite material microstructure for the one step generated and annealed device at 175°C for 10 minutes.

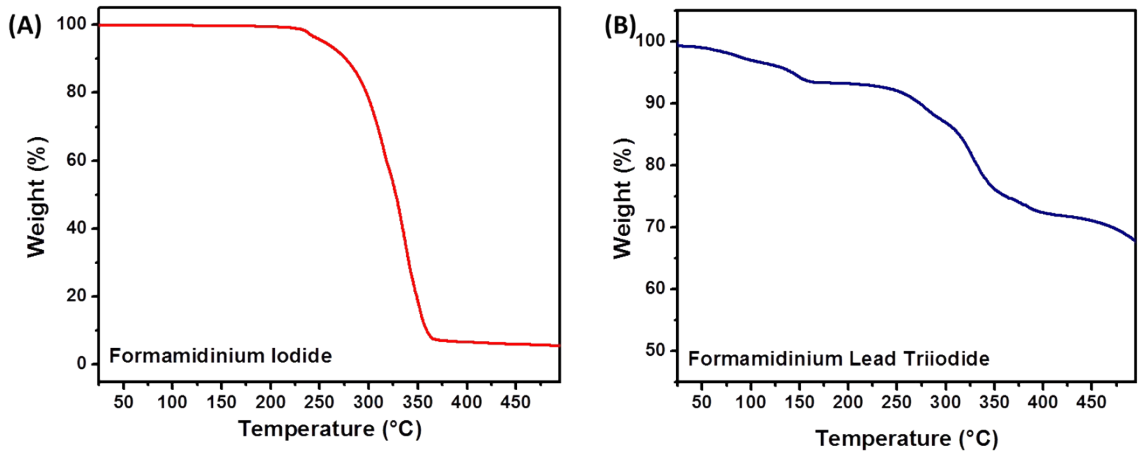

Figure S7 **(a)** Complementary thermogravimetric (TGA) analyses were performed on both formamidinium iodide (FAI-precursor material) and **(b)** formamidinium lead triiodide. Comparing the two materials, it is clear that the perovskite material is less stable and starts decomposing at lower temperature than the precursor.[5] Over the temperature range considered in this study, we can expect about a 10% weight loss of the perovskite to the atmosphere.

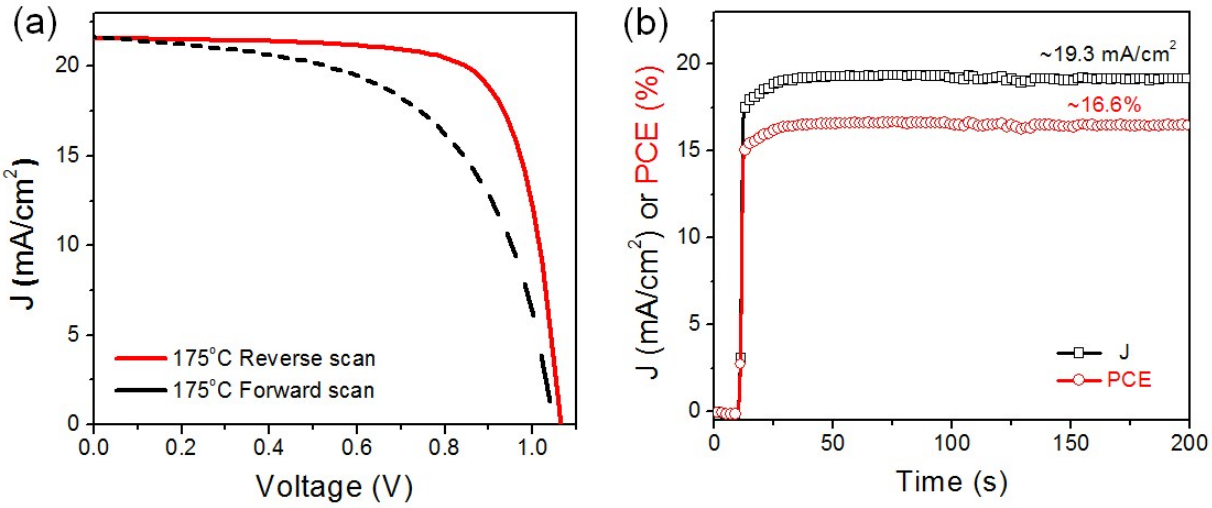

Figure S8: (a) Forward and reverse current density–voltage (J–V) curves for sequentially annealed device at 175˚C with the typical hysteresis behavior. For the reverse scan, the device shows a PCE of 17.09%, with J_{sc} of 21.58 mA/cm^2, V_{oc} of 1.07 V, and FF of 0.74. For the forward scan, the device shows a PCE of 13.18%, with J_{sc} of 21.65 mA/cm^2, V_{oc} of 1.05 V, and FF of 0.58. **(b)** Stabilized output of PCE and current density at maximum power point as a function of time for the same cell in (a) under simulated one-sun illumination.

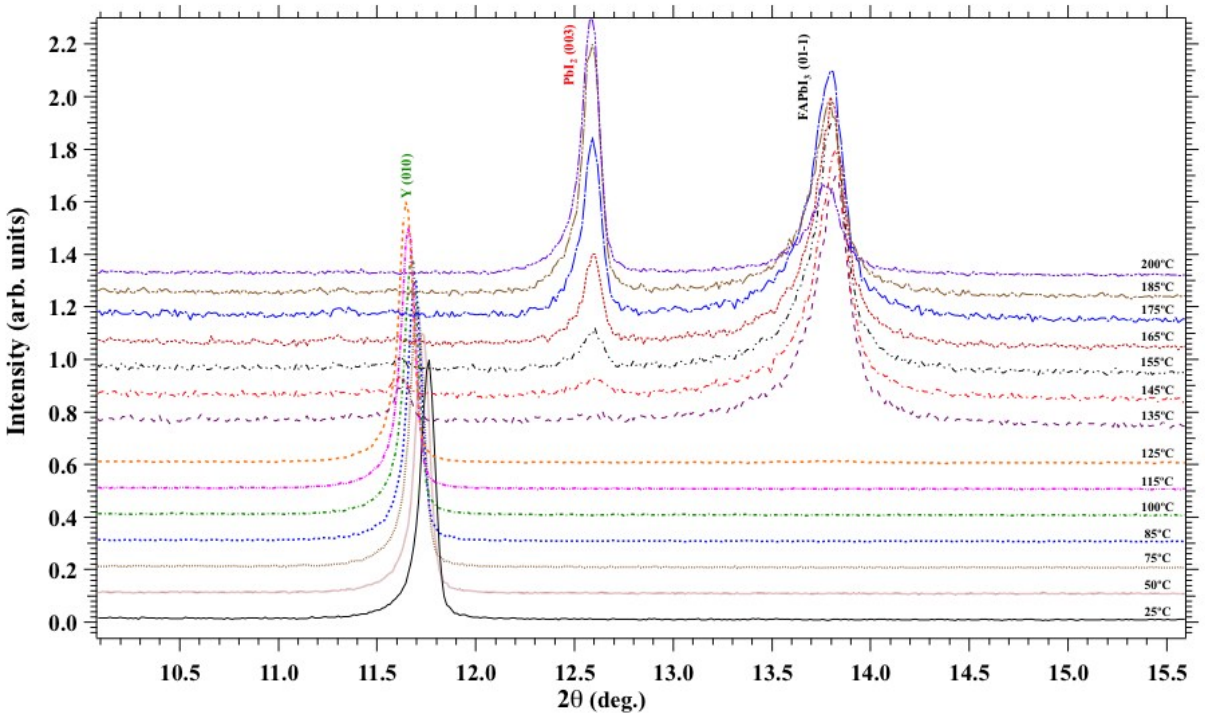

Figure S9: HTXRD scans in the 2**θ** region between 10 – 15.5° showing the emergence of the PbI_2 phase and the corresponding modifications to the $FAPbI_3$ phase.

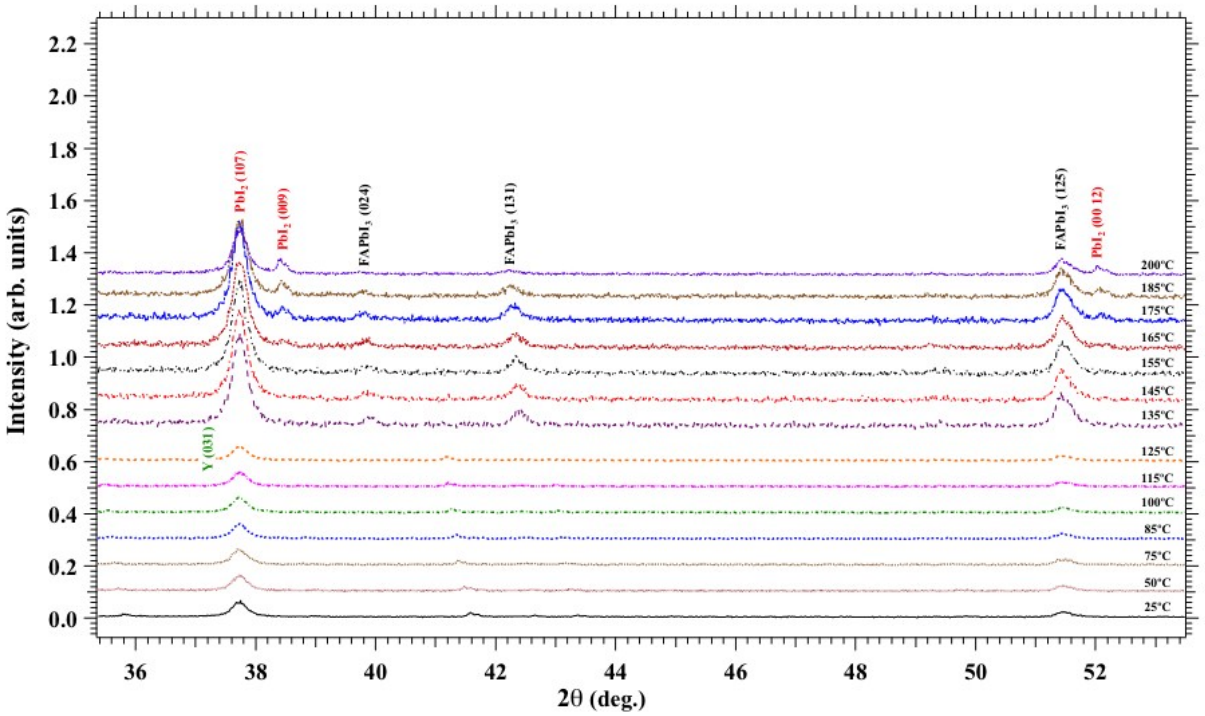

Figure S10: HTXRD scans in the 2**θ** region between 35.5 – 52.5° showing the emergence of the PbI_2 phase and the corresponding modifications to the $FAPbI_3$ phase.

Table S1: Measured device characteristics as function of annealing time. 175˚C was used as annealing temperature

Time (min)	J_{sc} (mA/cm^2)	V_{oc} (V)	FF (%)	PCE (%)
5	20.9	1.02	59.2	12.5
10	21.8	1.05	74.1	16.8
20	21.2	1.02	51.2	11.0
40	16.6	0.98	50.5	8.1

Table S2: Measured device statistics as function of temperature

Temperature (Deg C)		J_{sc} (mA/cm^2)	V_{oc} (V)	FF (%)	PCE (%)
150	average	19.54	1.045	62.4	12.74
	std	0.18	0.033	3.0	0.87
175	average	21.62	1.051	72.5	16.49
	std	0.26	0.013	1.7	0.59
200	average	20.28	1.041	67.7	14.29
	std	0.24	0.022	2.9	0.60
225	average	18.46	0.970	60.4	10.81
	std	0.24	0.036	3.3	0.66

Supplementary References

1 Egerton, R. F. & Takeuchi, M. Radiation damage to fullerite (C60) in the transmission electron microscope. *Applied Physics Letters* **75**, 1884-1886 (1999).

2 Krivanek, O. L. *et al.* Atom-by-atom structural and chemical analysis by annular dark-field electron microscopy. *Nature* **464**, 571-574, (2010).

3 Zobelli, A., Gloter, A., Ewels, C. P., Seifert, G. and Colliex, C. Electron knock-on cross section of carbon and boron nitride nanotubes. *Physical Review B* **75**, 245402 (2007).

4 Aguiar, J. A., Reed, B. W., Ramasse, Q. M., Erni, R. and Browning, N. D. Quantifying the low-energy limit and spectral resolution in valence electron energy loss spectroscopy. *Ultramicroscopy* **124**, 130 - 138 (2013).

5 Zhao, Y. and Zhu, K. Efficient Planar Perovskite Solar Cells Based on 1.8 eV Band Gap $CH_3NH_3PbI_2Br$ Nanosheets via Thermal Decomposition. *Journal of the American Chemical Society* **136**, 12241-12244 (2014).